

Expression of Complement Component 3 (C3) from an Adenovirus Leads to Pathology in the Murine Retina

Siobhan M. Cashman, Akshata Desai, Kasmir Ramo, and Rajendra Kumar-Singh

PURPOSE. Activation of complement has been implicated as one of the major causes of age-related macular degeneration (AMD). Evidence is accumulating for a role of complement in other retinal diseases, such as diabetic retinopathy and proliferative vitreoretinopathy. Because of the paucity of animal models that directly investigate the role of complement in retinal pathology, the authors sought to develop a model of increased complement expression and activation, specifically in the murine retina.

METHODS. The authors constructed a recombinant adenovirus-expressing murine complement component 3 (C3, AdcmvC3). Adult mice were injected in the subretinal space with either AdcmvC3 or a control virus, AdcmvGFP. After 1 to 2 weeks of exogenous C3 expression, mice were analyzed by scotopic electroretinography and fluorescein angiography. Eyes were harvested for histologic, immunohistochemical, and quantitative RT-PCR analyses.

RESULTS. Mice injected with C3-expressing adenovirus exhibited significantly increased vascular permeability, endothelial cell proliferation and migration, RPE atrophy, loss of photoreceptor outer segments, reactive gliosis, retinal detachment, and reduced retinal function relative to those injected with a control adenovirus. Deposition of the membrane attack complex was observed on endothelial cells and photoreceptor outer segments.

CONCLUSIONS. Adenovirus-mediated delivery of C3 to murine RPE induces significant functional and anatomic changes that reproduce many of the features of AMD as well as those of other retinal diseases. This novel model may be useful in assessing the role of complement in retinal pathology and in developing anti-complement therapies for retinal diseases associated with complement activation. (*Invest Ophthalmol Vis Sci.* 2011;52:3436–3445) DOI:10.1167/iovs.10-6002

Disregulation of the complement system is considered to be one of the major factors contributing to the etiology of age-related macular degeneration (AMD), one of the leading causes of blindness in the elderly.¹ The most devastating form of the disease, which affects approximately 10% of patients,² involves the growth of attenuated blood vessels from the chorioidal vasculature through Bruch's membrane and into the

retina. The plasma released by these "ill-formed" vessels damages photoreceptors and other retinal cells, eventually leading to a severe loss of vision. In the vast majority of AMD patients, however, extracellular deposits called *drusen* develop between the retinal pigment epithelium (RPE) and Bruch's membrane and eventually lead to atrophy of the RPE (geographic atrophy).

A potential role for complement in AMD was considered when complement proteins were identified in the drusen of AMD eyes.^{3–6} Since then, polymorphisms have been identified in a number of complement genes and have been observed to be either strongly predictive of or protective against AMD. A single amino acid change, Y402H, in factor H may account for as much as 40% to 50% of AMD in aging eyes.^{7–9} Haplotype variants in both factor B and complement component 2 (C2) present a significantly reduced risk for AMD,¹⁰ whereas an R80G substitution in complement C3 may increase the risk to as much as 22%.¹¹ The factor B (32Q) variant has been shown to have a fourfold lower binding affinity for C3b, with a reduced ability to form the convertase.¹² In addition, polymorphisms in C2, C3, and factor B have been shown to be significantly linked with progression to both types of advanced AMD, choroidal neovascularization, and geographic atrophy.^{2,13,14}

Although most of the evidence for complement-induced retinal pathology has been for AMD, indications of a role for complement activation in other retinal diseases is accumulating. Deposition of complement proteins has been observed in the choriocapillaris of patients with diabetic retinopathy¹⁵ and in the retinal vessels of diabetic subjects.¹⁶ These same vessels exhibited a significant reduction in expression of the complement regulatory proteins CD55 and CD59. Complement components have also been observed in the epiretinal membranes of patients with proliferative vitreoretinopathy (PVR)¹⁷ and upregulation of the classical pathway initiator protein C1q, and altered expression of other proteins of the cascade has been observed in glaucomatous eyes.^{18,19}

There are few animal models that directly investigate the role of complement in retinal function and pathology. Most of these have looked at the impact of different complement proteins in the development of laser-induced choroidal neovascularization (CNV) in the mouse retina. Some of these studies^{20–22} have demonstrated the dependence of this pathology on the alternative, rather than classical or lectin, pathway and on the formation of the membrane attack complex (MAC). Others²³ have demonstrated a significant role played by the anaphylatoxins C3a and C5a in the development of CNV. Aged mice with deficiency of factor H^{24,25} exhibit altered architecture in Bruch's membrane, RPE, and photoreceptors, reduced ERGs, and loss of integrity of retinal vessels. The alternative complement pathway has also recently been implicated as a major factor in light-induced retinal degeneration, which has been shown to be significantly reduced in a mouse deficient in factor D.²⁶ Ganglion cells of C3-deleted mice exhibit transient,

From the Department of Ophthalmology, Tufts University School of Medicine, Boston, Massachusetts.

Supported by The Ellison Foundation (RK-S), The Virginia B. Smith Trust (RK-S), the Lions Eye Foundation (departmental grant), and Research to Prevent Blindness (departmental grant).

Submitted for publication June 3, 2010; revised August 20 and December 10, 2010; accepted January 11, 2011.

Disclosure: S.M. Cashman, None; A. Desai, None; K. Ramo, None; R. Kumar-Singh, None

Corresponding author: Rajendra Kumar-Singh, Department of Ophthalmology, Tufts University School of Medicine, 136 Harrison Avenue, Boston, MA 02111; rajendra.kumar-singh@tufts.edu.

but significant, protection from degeneration caused by retinal ischemia reperfusion.²⁷

Although 1 of 3 distinct pathways—classical, lectin, or alternative—can initiate the complement cascade,²⁸ all three converge with the breakdown of C3 into its active components, C3a and C3b. This initiates the final part of the pathway that culminates in the formation of the MAC, a porelike structure that inserts in the membranes of self- or non-self cells, causing their lysis. In addition to the potential for cell lysis by the production of the opsonin C3b, the activation of C3 allows for the generation of the anaphylatoxins C3a and C5a, both of which are powerful and pleiotropic effectors of inflammation. Unlike the classical or lectin pathways, the alternative pathway is constantly active with small amounts of C3 hydrolysis and conversion to the convertase occurring in the serum. With the rapidly accumulating evidence implicating complement in a variety of retinal pathologic conditions, we considered it imperative to determine the effects of complement overexpression in the mouse retina. To do this, we elected to study the consequences of an increased local expression of C3 in the mouse retina on retinal anatomy and function. We hypothesized that a local increase in C3 expression would result in a local increase in C3 hydrolysis and conversion to the convertase. We increased the expression of C3 by injection of an adenovirus-expressing murine C3 regulated by the cytomegalovirus (CMV) promoter into the subretinal space. We have shown previously²⁹ that subretinal administration of a serotype 5 adenovirus containing a CMV-driven transgene results in transgene expression primarily in the RPE. Scotopic electroretinography, fluorescein angiography, and histologic analysis indicates that increased expression of C3 in the murine RPE causes significant functional and anatomic changes in the murine retina.

MATERIALS AND METHODS

Adenovirus Constructs

An *MluI* fragment from pCMV-Sport6C3 (image clone ID 5134713; American Type Culture Collection, Manassas, VA) containing a murine C3 cDNA was cloned into the *MluI* site of pShCMVMCS (a modified version of pShuttle containing the CMV promoter, an SV40 intron and polyA, and an *MluI*-inclusive multiple cloning site; details of this plasmid are available on request). The C3-containing pShuttle was then recombined with pAd-Easy1, and the rescued virus, AdCMVC3, was amplified as previously described.²⁹ The control virus used in this study, AdCMVGFP, has been previously described (EGFPNAd5³⁰). For Western blot analysis, human embryonic retinoblasts (HERs) were infected with either AdCMVC3 or AdCMVGFP in Dulbecco's modified Eagle's medium supplemented with 2% fetal bovine serum (Invitrogen, Carlsbad, CA). Cell lysate and media were loaded on a 10% Tris-HCl gel (Criterion; Bio-Rad, Hercules, CA). Membrane was probed with an anti-mouse C3 polyclonal antibody (1:1000; Cell Sciences, Canton, MA), followed by a 1:10,000 dilution of horseradish peroxidase-conjugated goat anti-rabbit. For immunocytochemistry, 1.2×10^6 HERs were infected at a multiplicity of infection of 600 and fixed with 4% formalin 24 hours after infection. Cells were incubated with a 1:50 dilution of anti-mouse C3 (MP Biomedicals, Solon, OH) followed by a 1:400 dilution of CY3-conjugated donkey anti-goat (Jackson ImmunoResearch Laboratories, West Grove, PA). Cells were imaged using an inverted microscope (IX51; Olympus, Tokyo, Japan) with appropriate filters, a digital camera (Retiga 2000R FAST; QImaging, Vancouver, BC, Canada), and software (QCapture Pro 5.0; QImaging).

Subretinal Administration of Viruses

All experiments involving animals were in conducted accordance with the ARVO Statement for the Use of Animals in Ophthalmic and Vision Research. C57Bl6/J mice were purchased from Jackson Laboratories

(Bar Harbor, ME) and were maintained in 12-hour dark/12-hour light cycles in accordance with federal, state, and local regulations. Injections were performed as previously described.²⁹ Briefly, mice were anesthetized by intraperitoneal injection of 0.1 mL/10 g ketamine (10 mg/mL)/xylazine (1 mg/mL), followed by application of 1 drop of proparacaine hydrochloride (0.5%) to each eye. Virus particles (2×10^9) were injected into the subretinal space of 6- to 8-week-old C57Bl6/J male mice using a transscleral/transchoroidal approach. In all mice, both eyes were injected with the same virus. One microliter of virus was administered using a 33-gauge needle and a 5- μ L glass syringe (Hamilton, Reno, NV).

Scotopic Electroretinography

After overnight dark adaptation, mice were anesthetized as described. This was followed by the application of one drop of 1% tropicamide (Akorn, Inc., Lake Forest, IL) to each eye for pupil dilation. Body temperature of the mouse was maintained using an animal temperature controller (ATC 1000; World Precision Instruments, Sarasota, FL). ERGs were recorded at two different light intensities (-10 and 0 dB) using (UTAS Visual Diagnostic Test System with Big Shot LED Ganzfeld; LKC Technologies, Gaithersburg, MD) using contact lens electrodes (LKC Technologies). Ten flashes were recorded and averaged for each light intensity.

Tissue Harvest, Processing, and Staining

Eyes were fixed overnight in 4% paraformaldehyde and dehydrated in 15% to 30% sucrose in 0.1 M phosphate buffer. Cornea, lens, and iris were removed, and eyecups were embedded in compound (Tissue-Tek; Adwin Scientific Industrial, Tryon, NC). Sections measuring 14 μ M were taken using a cryostat (Microm 550; Thermo Scientific, Pittsburgh, PA).

GSL I. Sections were incubated at 37°C for 10 minutes with 500 μ g/mL BSA in PBS followed by 100 μ g/mL FITC-conjugated *Griffonia simplicifolia* Lectin I (Isolectin B4; Vector Laboratories, Burlingame, CA) in PBS for 1 hour at 37°C. Eyecups (with retinas removed before fixation) were stained as for sections, except that blocking was performed for 30 minutes with 2.5 mg/mL BSA in PBS. Four relaxing cuts were administered before mounting on slides. Sections adjacent to those with representative GSL I stain for each of AdcmvC3 and AdcmvGFP-injected were stained for the following:

DAPI. Sections were pretreated with 0.05% Triton-PBS (PBST) for 15 minutes, followed by 1 μ g/mL DAPI in PBS for 5 minutes at room temperature (RT).

Rhodopsin. After blocking with 6% normal donkey serum (Jackson ImmunoResearch) in 0.25% PBST for 1 hour at RT, sections were incubated for 2.5 hours with a 1:250 dilution of mouse monoclonal 1D4 (kind gift of Robert Molday) in blocking buffer at RT, followed by a 1.5-hour incubation at RT with a 1:400 dilution of CY3-conjugated goat anti-mouse (Jackson ImmunoResearch).

GFAP. Staining was performed as for rhodopsin, with a 1:500 dilution of rabbit polyclonal antibody anti-gliofibrillary acidic protein (GFAP; Novus Biologicals Inc, Littleton, CO) followed by a 1:500 dilution of CY3 goat anti-rabbit (Jackson ImmunoResearch), both in 6% normal goat serum.

MAC. After blocking with 6% normal goat serum in 0.3% PBST for 30 minutes at RT, sections were stained for 2.5 hours at RT with a 1:200 dilution of rabbit anti-mouse C9 antibody (kind gift of B. Paul Morgan) in PBST, followed by 1:400 dilution of CY3-conjugated goat anti-rabbit (Jackson ImmunoResearch) at RT for 1 hour. In all cases, specificity of antibodies was determined using control antibodies of the same isotype. Sections and flatmounted eyecups were imaged using an inverted microscope (IX51; Olympus) with appropriate filters, a digital camera (Retiga 2000R FAST; QImaging), and software (QCapture Pro 5.0; QImaging).

Retinal Detachment

To produce prolonged retinal detachment without adenovirus, 6- to 8-week-old C57Bl6/J mice were injected with 1 μ L of 0.25% sodium hyaluronate.³¹ Nine days after injection, eyes were harvested and fixed with 4% paraformaldehyde, and cryosections were stained with FITC-GSL I as described. For AdcmvC3-injected and AdcmvGFP-injected eyes, detachment was calculated by counting the number of sections with retinal detachment and multiplying by the thickness of each section (14 μ M). Data were analyzed using an unpaired Student's *t*-test.

Fluorescein Angiography

Mice were anesthetized as described, and one drop of 1% tropicamide was added to each eye. 200 μ L of 2.5% sodium fluorescein (Akorn, Inc.) in 1 \times PBS was injected intraperitoneally. Eyes were coated with 2% methylcellulose and a coverslip (Corning, No.1) used to image retinal vessels using a Nikon C-PS160 dissecting microscope and appropriate filters. Eyes were monitored for 3 to 10 minutes, and images were captured (DP20; Olympus) 5 minutes after the injection of sodium fluorescein.

Quantitative RT-PCR

Eyes were harvested, and the cornea, lens, iris, and optic nerve were removed. The remaining tissue was placed in reagent (RNA Stat-60; Tel-Test, Inc., Gainesville, FL) and was homogenized using a homogenizer (AHS200; VWR, Buffalo Grove, IL). Total RNA was purified in accordance with the manufacturer's instructions and was treated for DNA contamination using a DNA-free kit (Turbo; Applied Biosystems, Foster City, CA). Total RNA was assayed for C3, VEGF, and β -actin using a one-step RT-PCR kit (iScript; Bio-Rad) and the Applied Biosystems assays (mouse C3, Mm00437858_m1; mouse VEGF, Mm00437304_m1; mouse β -actin, part 4352663) on a multicolor real-time PCR detection system (iQ5; Bio-Rad) and was analyzed using optical system software (iQ5; Bio-Rad).

Statistical Analysis

All analyses were performed using statistical software (Prism 5; GraphPad Software, Inc). In those experiments comparing three conditions, data were analyzed using a one-way ANOVA with a post-Newman-Keuls multiple comparison test for significance. All other data were analyzed using an unpaired Student's *t*-test. For qRT-PCR, a *t*-test was performed in which uninjected (for the purpose of determining significance) was given the hypothetical value of 1.0, and the significance of the fold difference of C3 and GFP was measured relative to this value.

RESULTS

C3 Expression In Vitro

C3 is a secreted protein produced as a single polypeptide precursor, pro-C3, with a predicted molecular weight of 170 kDa. Pro-C3 is cleaved intracellularly to form C3, which consists of an α (107-kDa) and a β (62-kDa) chain joined by disulfide bonds.^{32,33} Expression of C3 from AdcmvC3 was confirmed by immunostaining of infected HERs (Fig. 1a). Unlike the distribution of GFP in the control AdcmvGFP-infected cells, which exhibits a diffuse presence throughout the nucleus and cytoplasm, C3 staining in the AdcmvC3-infected cells was observed to be primarily cytoplasmic. To confirm the correct size and processing of C3, a Western blot analysis was performed for both lysate and media of HERs infected with AdcmvC3 (Fig. 1b). Under nonreducing conditions, two bands were observed in the lysate of AdcmvC3-infected cells. The approximate sizes of these bands were consistent with the presence of both C3 and its precursor, pro-C3. As expected, only the processed C3 band was observed in the media. Under

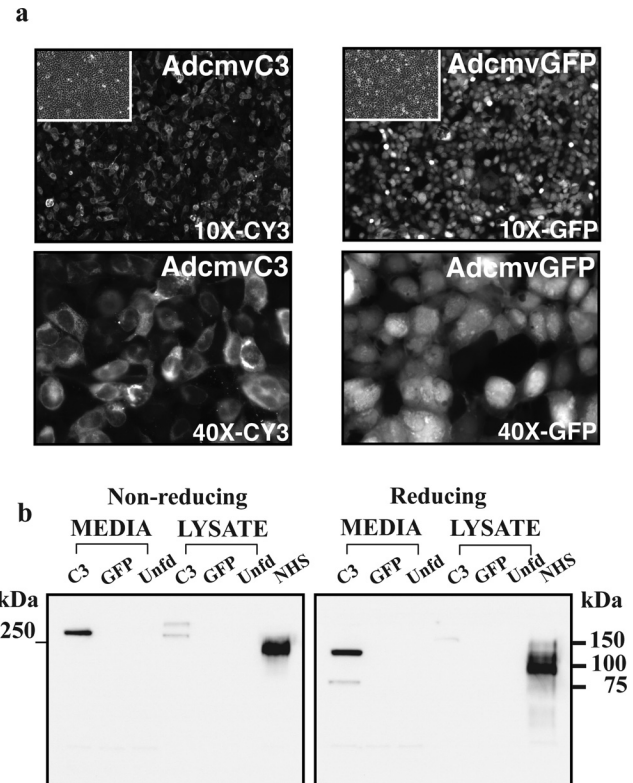
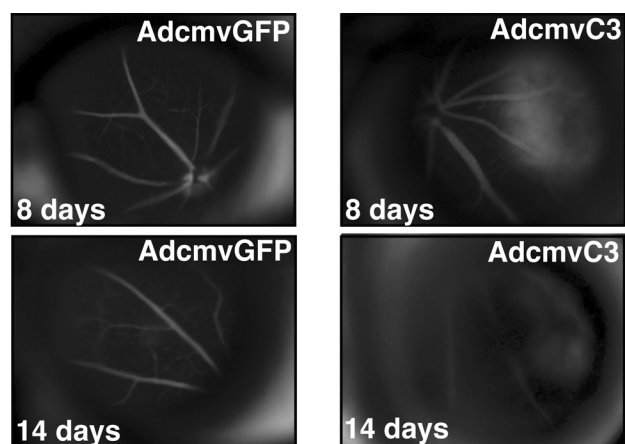


FIGURE 1. Correct processing and efficient secretion of C3 expressed from adenovirus in vitro. (a) Immunostaining of human embryonic retinoblasts infected with either AdcmvC3 or AdcmvGFP. GFP is observed in the nucleus and cytoplasm of AdcmvGFP-infected cells (GFP filter), whereas C3 staining is observed primarily in the cytoplasm of AdcmvC3-infected cells (CY3 filter). Bright-field images are shown in the insets. (b) Western blot analysis of similarly infected cells shows correct processing of C3 intracellularly and efficient secretion into the media. Under *non-reducing* conditions, the disulfide-linked α and β chains of C3 are observed in the media and lysate of AdcmvC3-infected cells. Under *reducing* conditions, the α and β chains in the media migrate separately, consistent with their predicted molecular weights (107 and 62 kDa, respectively). Unfd, uninfected; NHS, normal human serum.

reducing conditions, two bands consistent with the α and the β chain were observed in the media. The lysate contained a faintly higher molecular weight band consistent with nonreduced C3.

Increased Permeability of Blood Vessels in the Presence of High Levels of C3

One of the key features of a large proportion of AMD eyes is the spontaneous growth of new and leaky choroidal and retinal blood vessels.³⁴ Fluorescein angiography was performed on mice injected with adenoviruses expressing either C3 or GFP into the subretinal space both 8 and 14 days postinjection (PI). Although none of the eight AdcmvGFP-injected eyes (GFP-injected) tested showed any evidence of leakiness at 8 days PI, 2 of 8 (25%) AdcmvC3-injected (C3-injected) eyes showed fluorescein leakage (Fig. 2) at this time point. At 14 days PI, rapid diffusion of fluorescein into the vitreous was observed in all five (100%) of the C3-injected eyes tested (Fig. 2), to the extent that the smaller retinal vessels were no longer visible. None of the four GFP-injected eyes tested at the 14 day time point showed any leakiness.



Number of eyes exhibiting fluorescein leakage

	AdcmvGFP	AdcmvC3
8 Days Post Injection	0% (0/8)	25% (2/8)
14 Days Post Injection	0% (0/4)	100% (5/5)

FIGURE 2. Loss of blood vessel integrity in mice injected with AdcmvC3. Fluorescein angiography shows discrete regions of leakage in AdcmvC3-injected eyes 8 days after injection, with rapid leakage of fluorescein occurring 14 days after injection. No leakage was observed in the control, AdcmvGFP-injected, mice at either time point. $n = 8$ for AdcmvC3, AdcmvGFP (8 days); $n = 5$ for AdcmvC3, $n = 4$ for AdcmvGFP (14 days).

C3 Overexpression Results in Extensive Proliferation of Endothelial Cells

Neovascularization is typically preceded by the proliferation and migration of vascular endothelial cells.³⁵ To determine the occurrence and location of endothelial cell proliferation, C3-injected or GFP-injected eyes were harvested 9 days PI, and cryosections were stained using the endothelial cell marker GSL I, isolectin B4 conjugated to FITC. Before GSL I staining, cryosections of GFP-injected eyes were assessed for GFP expression (Fig. 3a). Although the extent of GFP expression varied between injections, expression was only observed in the RPE cell layer. After staining with GSL I, C3-injected eyes exhibited extensive staining throughout the retina compared with GFP-injected eyes (Fig. 3b). Increased GSL I staining was seen in the region of injection in the choroid of GFP-injected compared with uninjected eyes (uninjected eyes not shown; Fig. 3b). In addition, an increase in staining in the retina in the region of injection was observed in approximately 50% of GFP-injected mice compared with uninjected (uninjected eyes not shown) but was much less intense than in C3-injected eyes and limited to the inner retina. At higher magnification, C3-injected eyes were observed to have GSL I-positive cells at the RPE/retinal interface and in all layers of the retina (Fig. 3c). Unlike C3-injected eyes, the increased GSL I staining in the GFP-injected eyes was restricted primarily to the choroid with some increased staining in the retina (Fig. 3c).

A comparison of bright-field images with those of FITC-GSL I indicated a disruption of the RPE/choroid within the region of GSL I staining in C3-injected eyes (Fig. 4a). In a number of eyes (2 of 6), we observed a migration of pigmented cells into the retina (Fig. 4a, inset). In GFP-injected eyes, the integrity of the RPE cells was maintained, with the GSL I-positive endothelial cells not breaching the RPE (Fig. 4a). Closer examination of the RPE/choroid of C3-injected retinas indicates a loss of RPE cells

and a loss of pigment, with cells in this region staining positively for GSL I (Fig. 4b).

Increased Retinal Detachment Is Observed in AdcmvC3-Injected Eyes

To quantitate the extent of endothelial cell proliferation in C3-injected eyes compared with that observed in GFP-injected, eyecups (with retina removed) were stained with FITC-GSL I (Fig. 5a). The C3-injected eyecups were observed to have a significantly greater area of GSL I staining ($0.73 \pm 0.17 \text{ mm}^2$;

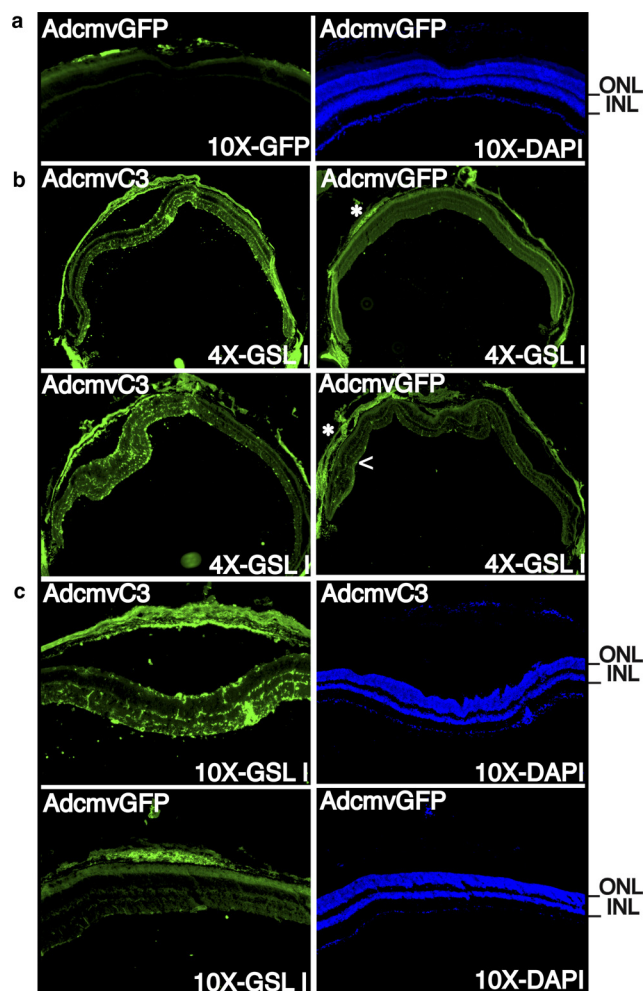


FIGURE 3. Proliferation and migration of endothelial cells in AdcmvC3-injected retinas. (a) Expression from AdcmvGFP was observed exclusively in the RPE. (b) Low-magnification images (4X) show intense FITC-GSL I staining, particularly in the area of detachment, in AdcmvC3-injected retinas compared with the control, AdcmvGFP-injected. Representative images from two independent injections for each virus are shown. GSL I staining is observed in the choroid (*) of all AdcmvGFP-injected eyes. Increased GSL I staining is also observed in the retina of some AdcmvGFP-injected mice close to the site of injection (<) but is much reduced compared with AdcmvC3-injected. It should be noted that (as for AdcmvC3-injected) AdcmvGFP-injected retinas were stained across the region of injection, including the area of GFP-positive RPE cells. AdcmvGFP sections shown for FITC-GSL I stain do not contain GFP-positive RPE cells but are representative of GSL I stain across the region of injection. (c) Higher magnification images show strong GSL I stain at the RPE/retinal junction and throughout the retina, in AdcmvC3-injected mice. GSL I binding is observed, primarily in the choroid within the region of injection in AdcmvGFP-injected mice. ONL/INL, outer/inner nuclear layer. $n = 6$ for AdcmvGFP and AdcmvC3.

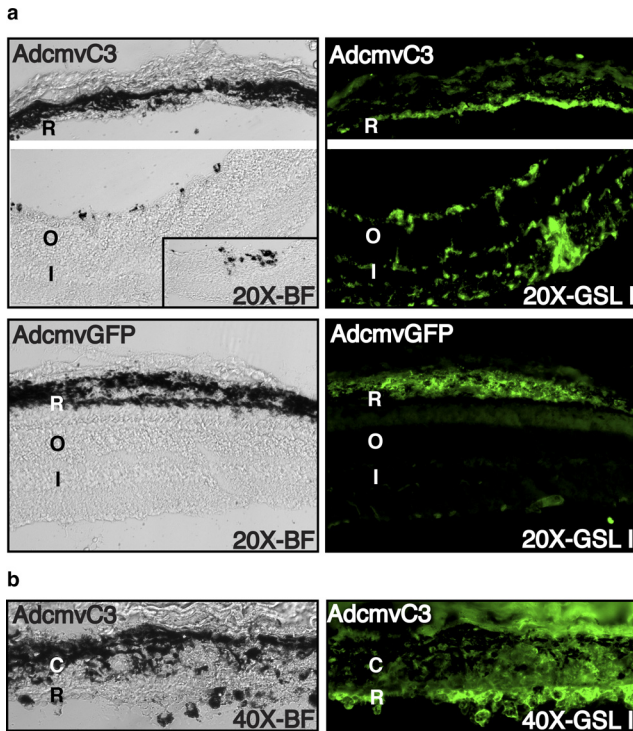


FIGURE 4. Disruption of RPE and choroid in AdcmvC3-injected eyes. **(a)** Images illustrate disruption to the RPE/choroid of AdcmvC3-injected mice, with cells in this region staining positive for GSL I. In a number of eyes (2 of 6), pigmented cells could be observed migrating into the retina (*inset*). In AdcmvGFP-injected eyes, GSL I stain is restricted mostly to the choroid, with the RPE cell layer remaining intact. **(b)** Closer examination of AdcmvC3-injected retinas indicates a loss of RPE cells and pigment along the region of GSL I staining. BF, bright-field; O, outer nuclear layer; I, inner nuclear layer; C, choroid. $n = 6$ for AdcmvGFP and AdcmvC3.

$P < 0.05$) than GFP-injected eyecups (0.03 ± 0.02 mm²; Fig. 5b).

Retinal detachment was observed within the region of the most intense lectin staining in all C3-injected eyes (Fig. 3b). Quantitation of the extent of retinal detachment observed in both GFP-injected and C3-injected mice demonstrated that the extent of retinal detachment in C3-injected retinas was significantly greater (2.6-fold; $P < 0.05$) than that observed in GFP-injected mice (Fig. 5c). To determine whether the increased endothelial cell staining and disruption of the RPE/choroid observed in C3-injected mice could be accounted for solely by the greater amount of retinal detachment, 0.25% sodium hyaluronate was injected into the subretinal space of mice to induce a prolonged retinal detachment.³¹ Nine days after injection, eyes were harvested and fixed, and cryosections were stained with GSL I. GSL I staining was observed almost exclusively in the inner nuclear layer (INL; Fig. 5d), with a small number of pigmented cells at the RPE/retinal interface staining positively for GSL I. Increased magnification of the RPE/choroid in one of the sodium hyaluronate-treated eyes reveals an intact RPE layer (Fig. 5e). No GSL I staining was observed in this region (data not shown). This observation suggested that the increased endothelial cell staining and disruption of the RPE/choroid observed in C3-injected mice was due to the expression of C3 and not to greater retinal detachment.

Photoreceptor Degeneration and Müller Cell Reactivity in C3-Injected Retinas

Staining of C3-injected retinas with the nuclear stain DAPI indicated a definitive perturbation of the outer nuclear layer

(ONL), whereas the INL remained relatively undisturbed (Fig. 6a). TUNEL staining of C3-injected retinas was negative (data not shown), indicating little or no apoptosis in the ONL. To further investigate the integrity of photoreceptors, we stained retinal sections for rhodopsin and confirmed the loss of outer segments in C3-injected eyes (Fig. 6b). Most of the rhodopsin in GFP-injected and uninjected retinas was localized in the outer segments, with very little staining in the ONL.

In many retinal diseases, Müller cells become activated,³⁶ a phenomenon that can be viewed by investigating the expression of GFAP. In C3-injected eyes, the activation of Müller glia was confirmed by the observation of GFAP throughout the Müller cell, extending from the inner to the outer limiting membrane (Fig. 6c). It is noteworthy that there were also pockets of little or no staining within this region. This staining pattern was observed only in the area of detachment. GFAP staining was observed extending into the inner plexiform and nuclear layers of the GFP-injected eyes, suggesting some reactivity in these retinas. As expected, in the uninjected retinas, GFAP staining occurred in astrocytes and Müller cell endfeet at the inner limiting membrane.

Increased C3 Expression Results in Reduced Retinal Function

Eight days after injection, scotopic electroretinograms were recorded at two different light intensities, -10 dB and 0 dB. At

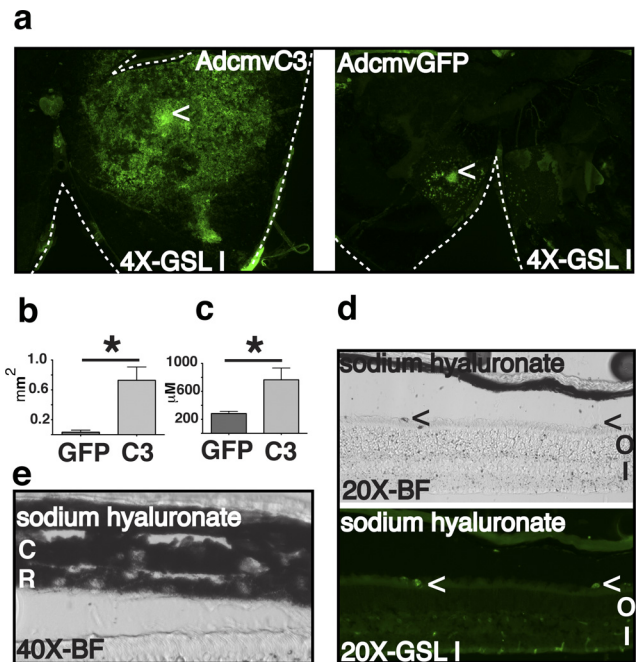


FIGURE 5. Increased retinal detachment in AdcmvC3-injected eyes. **(a)** FITC-GSL I stain of AdcmvC3- and AdcmvGFP-injected eyecups. Increased staining is observed for both viruses at the site of injection (<), but staining in AdcmvC3-injected eyes extends beyond the region of injection. Dotted lines delineate the border of the eyecups. **(b)** Quantitation of GSL I staining shows a significantly greater area of staining in AdcmvC3-injected eyecups relative to those injected with AdcmvGFP ($*P < 0.05$). AdcmvC3 ($n = 13$), AdcmvGFP ($n = 6$). **(c)** Retinal detachment is significantly increased (2.6-fold) in AdcmvC3-injected eyes relative to AdcmvGFP-injected ($*P < 0.05$). AdcmvC3 ($n = 5$), AdcmvGFP ($n = 4$). **(d)** GSL I stain of eyes injected with 0.25% sodium hyaluronate shows staining confined to endothelial cells of the inner nuclear layer, with a few pigmented cells at the RPE/retinal interface (<) staining GSL I-positive ($n = 3$). **(e)** Higher magnification of the RPE/choroid of another eye injected with sodium hyaluronate shows an intact RPE cell layer. BF, bright-field; C, choroid; R, RPE; O, outer nuclear layer; I, inner nuclear layer.

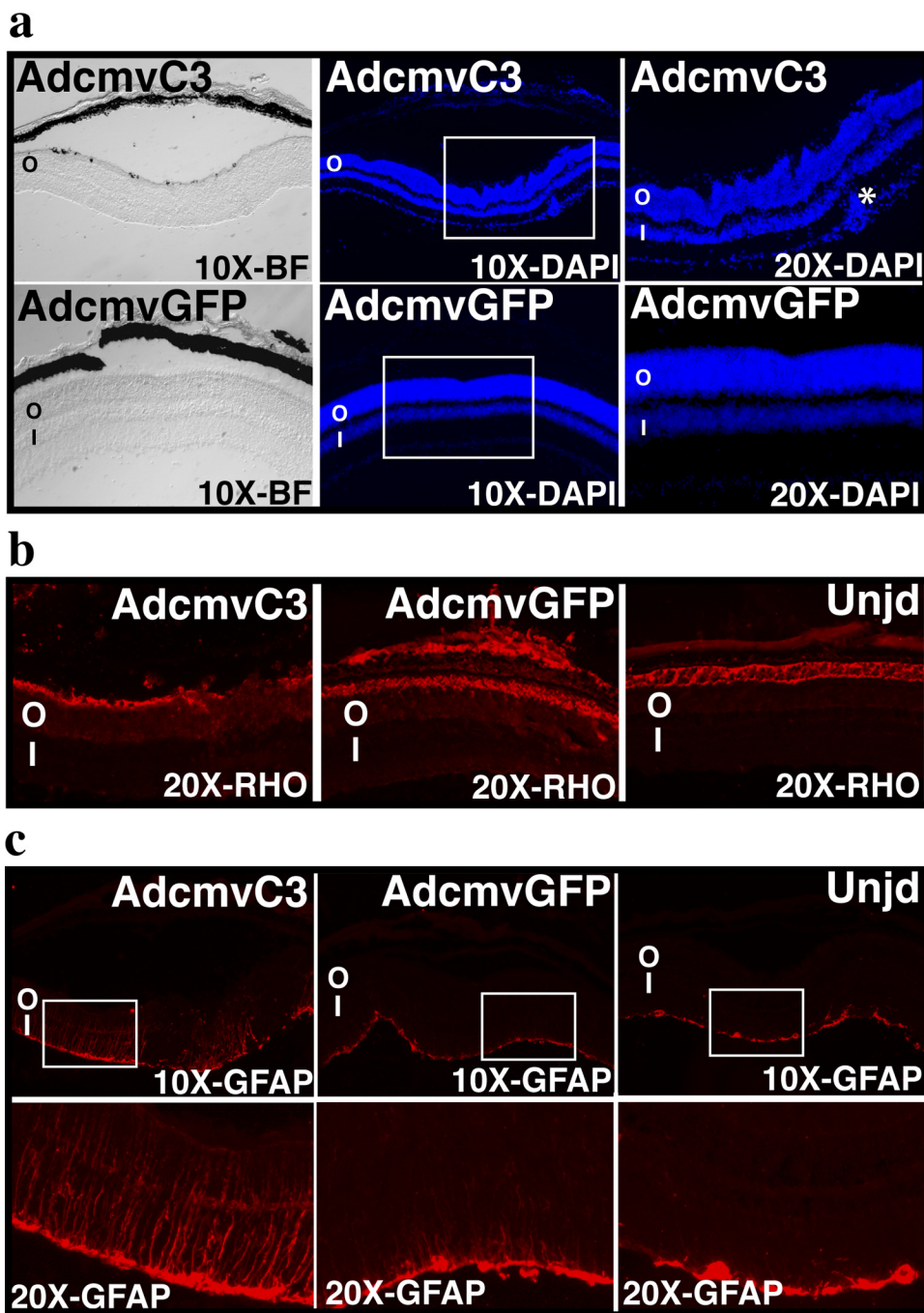


FIGURE 6. Disturbance of the outer nuclear layer, outer segment loss, and Müller cell activation in AdcmvC3-injected retinas at 9 days after injection. **(a)** DAPI stain shows perturbations in the photoreceptor cell layer, with little or no disturbance to the inner nuclear layer, in AdcmvC3-injected retinas. Proliferation of cells can also be seen in the ganglion cell and inner plexiform layers (*). Higher magnification of boxed regions are shown. **(b)** Rhodopsin (RHO) staining showing a loss of outer segments in AdcmvC3-injected retinas. RHO staining was observed predominantly in the outer segments of AdcmvGFP-injected and uninjected retinas. Some nonspecific staining is seen in the sclera of some animals. **(c)** An altered distribution of GFAP can be seen in the Müller cells of AdcmvC3-injected retinas, in which it extends throughout the Müller cell (from inner to outer limiting membranes). A change in GFAP localization can be observed in Müller cells in AdcmvGFP-injected retinas in which it extends toward the outer retina. GFAP is typically localized to astrocytes and to the endfeet of nonreactive Müller cells at the inner limiting membrane, as seen in uninjected retinas. Higher magnifications of boxed regions are shown below. BF, bright-field; O, outer nuclear layer; I, inner nuclear layer; Unjd, uninjected. $n = 4$ for AdcmvGFP and AdcmvC3.

both intensities, b-wave amplitudes were observed to be significantly reduced in C3-injected eyes relative to GFP-injected or uninjected eyes ($P < 0.05$; Fig. 7). B-wave amplitudes of C3-injected mice were reduced by $29.8\% \pm 7.4\%$ (0 dB) and $21.5\% \pm 7.1\%$ (−10 dB) when compared with GFP-injected mice. A-wave amplitudes were also observed to be significantly reduced in C3-injected eyes at the higher light intensity (0 dB) when compared with both uninjected and GFP-injected ($P < 0.05$) eyes (Fig. 7) but were not reduced at the lower light intensity (−10 dB). Relative to GFP-injected eyes, a-waves of C3-injected mice at 0 dB were observed to be reduced by $18.4\% \pm 7.3\%$. The ratio of b-wave to a-wave was also reduced ($15.5\% \pm 3.9\%$) significantly in C3-injected mice when compared with GFP-injected eyes at the higher light intensity (0 dB, $P < 0.05$) but not at the lower light intensity (−10 dB). No

significant reduction was observed in retinal function for GFP-injected compared with uninjected mice.

C3-Injected and GFP-Injected Retinas Differ in Their Expression of C3 and VEGF

Eight days after injection, C3- and GFP-injected eyes were examined for levels of C3 expression. Because of the significant amount of endothelial cell staining in C3-injected eyes, we chose to simultaneously assay for VEGF mRNA expression. Expression of C3 mRNA was significantly increased in both C3-injected eyes (57.0 ± 11.8 -fold; $P < 0.01$) and GFP-injected eyes (6.2 ± 1.2 -fold; $P < 0.01$) compared with uninjected eyes (Fig. 8). Surprisingly, however, though C3-injected eyes showed little or no change in VEGF expression (0.97 ± 0.14 -

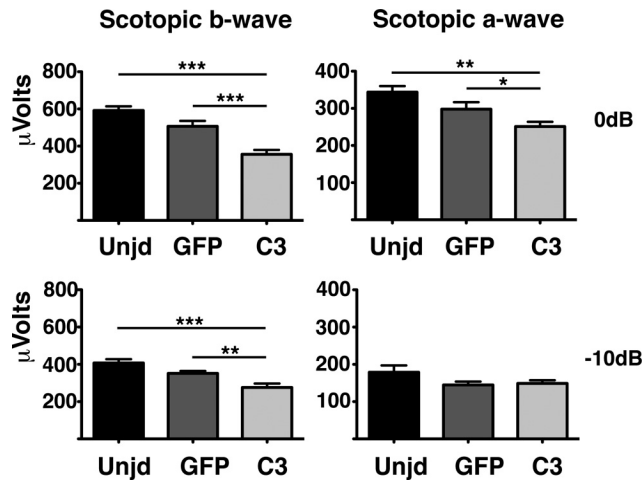


FIGURE 7. Electroretinograms are significantly reduced in AdcmvC3-injected retinas. B-wave amplitudes of AdcmvC3-injected retinas are observed to be significantly reduced at both higher and lower light intensities relative to both AdcmvGFP-injected and uninjected, whereas a-wave amplitudes were observed to be significantly impaired only at the higher light intensity (0 dB). No significant reduction was observed in retinal function for AdcmvGFP-injected mice relative to uninjected. Data are presented as the mean ± SE. *n* = 24 for each of AdcmvGFP- and AdcmvC3-injected eyes. *n* = 8 for uninjected.

fold change), GFP-injected eyes had a significant 2.6 ± 0.5-fold increase in VEGF expression (*P* < 0.05) compared with uninjected eyes (Fig. 8). We considered the possibility that VEGF mRNA levels might have increased at an earlier time point in C3-injected eyes, and we examined the expression of both mRNAs in whole eyecups at 3 days after injection. At this time point, we observed a significant increase in VEGF mRNA levels in C3-injected eyes of 2.98 ± 0.62-fold above uninjected eyes (Fig. 8; *P* < 0.05). The expression of VEGF in GFP-injected eyes was also significantly elevated above uninjected eyes (1.67 ± 0.21-fold) at this time point (*P* < 0.05). Interestingly, both GFP-

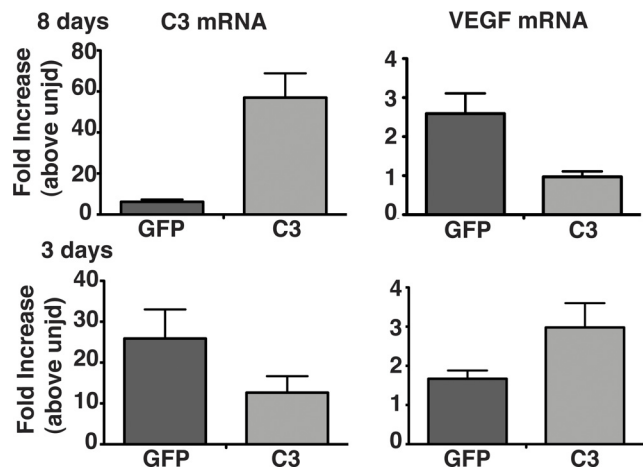


FIGURE 8. Expression of C3 mRNA, but not VEGF mRNA, is increased in AdcmvC3-injected retinas relative to uninjected. At both 3 and 8 days after injection, expression of C3 mRNA was significantly increased in AdcmvC3-injected retinas. Although no change in VEGF mRNA was observed in AdcmvC3-injected mice at 8 days after injection, a significant increase was observed at the 3-day time point. At this time point, however, a significant increase is also observed in AdcmvGFP-injected compared with uninjected retinas. Data are presented as the mean ± SE. Unj, uninjected. *n* = 6 for AdcmvGFP and AdcmvC3; *n* = 12 for uninjected.

and C3-injected eyes had significantly increased C3 mRNA expression compared with uninjected eyes at this time point (Fig. 8; *P* < 0.05). Although the levels of C3 mRNA in GFP-injected eyes were 25.9 ± 7.1-fold higher than in uninjected eyes while those of C3-injected eyes were observed to be 12.65 ± 4.02-fold higher than the levels measured in uninjected eyes, this apparent difference between GFP-injected and C3-injected eyes was not significant.

Deposition of Membrane Attack Complex in AdcmvC3-Injected Retinas

To determine whether complement was activated in C3-injected eyes, retinas harvested 9 days PI were stained using a polyclonal antibody to mouse C9 (Fig. 9). Membrane attack complex (MAC) deposition could be observed on cells at the RPE/retinal interface (Fig. 9a); these cells also stained positively

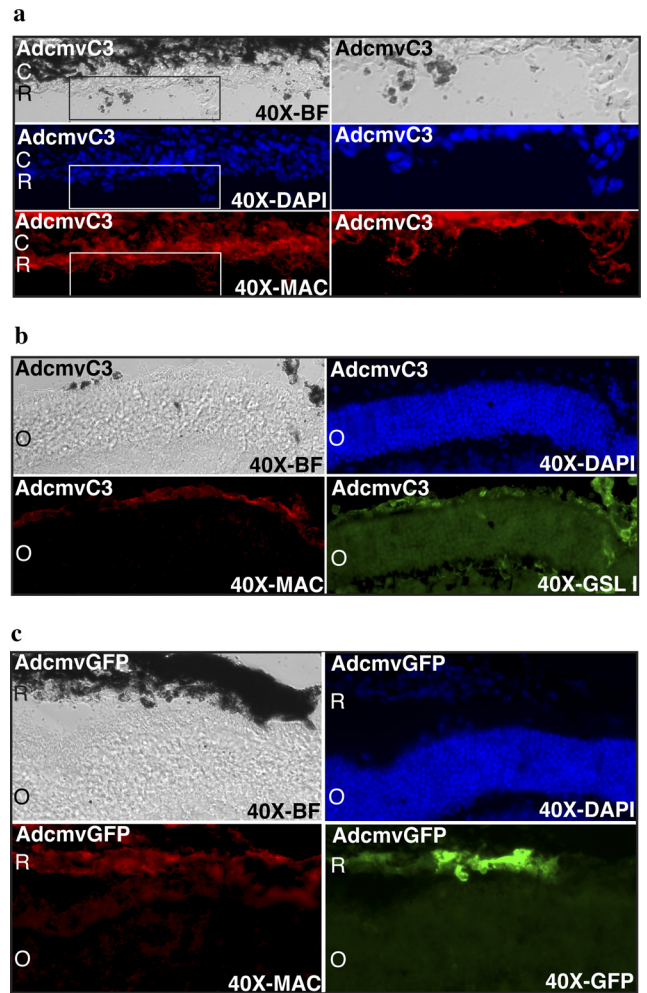


FIGURE 9. AdcmvC3-injected retinas exhibit MAC deposition on endothelial cells and outer segments. (a) Staining of AdcmvC3-injected retinas for MAC shows deposition of the protein complex on cells at the RPE/retinal interface. These cells also stain positive for GSL I (not shown). Higher-magnification images of boxed regions show punctate staining characteristic of MAC. (b) MAC staining is also observed on the remaining outer segments of the photoreceptors. (c) Staining of AdcmvGFP-injected retinas shows staining in transduced RPE cells at the site of injection but no staining in the retina. As expected after subretinal injection, some disruption of the RPE/choroid was noted at the site of injection in these mice. MAC staining was also observed in the choroid coincident with GSL I staining (not shown). BF, bright-field; C, choroid; R, RPE; O, outer nuclear layer.

for FITC-GSL I (data not shown). A higher magnification image of these GSL I-positive (GSL I staining not shown) endothelial cells at the RPE/retinal interface reveals more clearly the punctate membrane staining characteristic of MAC deposition. In addition, strong staining could be observed on the remaining outer segments of the photoreceptors (Fig. 9b). In GFP-injected retinas, MAC staining was observed in the choroid (coincident with GSL I stain [not shown]). MAC staining was also observed on some of the AdcmvGFP-transduced RPE cells (Fig. 9c) at the site of injection but was not observed on neighboring RPE cells or in the retina.

DISCUSSION

With increasing evidence of the role of complement in the etiology of AMD and in other retinal diseases, there has been a lot of interest in studying the effects of complement dysregulation on the health of the retina. Much of the investigation has centered around the impact of inhibitors of complement, such as factor H and CD59, on the development of choroidal neovascularization in response to laser-induced damage of Bruch's membrane.^{20–22,37} A recent study of aged mice deficient in factor H has shown the deposition of C3 and C3b in the retinal vasculature, resulting in attenuation of retinal vessels and reduced blood flow.²⁵ We chose a more direct approach, involving the study of the consequences of local C3 overexpression in the RPE of the murine retina. We hypothesized that increased expression of C3 in murine RPE could lead to increased local C3 hydrolysis, convertase production, and complement activation. Adenovirus expressing either murine C3 or GFP from a CMV promoter was injected into the mouse subretinal space. Between 8 and 14 days after injection, eyes were analyzed to determine the effect of local exogenous C3 production.

A large proportion of patients with advanced AMD present with a spurious growth of new blood vessels from the choroid into the subretinal space,² and a significant subset of neovascular patients present with new vessels originating from the inner retina.³⁴ These immature blood vessels leak fluid, causing retinal detachment and degeneration. The relationship between complement activation and growth of new and "leaky" blood vessels in AMD eyes is unclear. In animal models it has been found that regulators of complement, such as factor H and CD59, can significantly reduce neovascularization in the laser-induced model of CNV.^{20,37} In addition, mice deficient in receptors for C3a and C5a exhibit significantly reduced laser-induced endothelial cell proliferation.²³ The anaphylatoxin C3a is known to increase vascular permeability through structural changes in the endothelium.²⁸ C5b-9 has been shown to affect endothelial cell proliferation and migration in models of atherosclerosis³⁸ and to induce the release of growth factors such as basic fibroblast growth factor.³⁹ Our study indicates that local exogenous expression of C3 can induce both leakiness of blood vessels and proliferation of endothelial cells in the murine retina. C3-injected eyes exhibit signs of leakage as few as 8 days after administration of the virus, a time at which a significant amount of endothelial cell staining is also observed throughout the choroid and retina. Deposition of MAC was evident on endothelial cells at the RPE-retinal interface and on remnants of the photoreceptor outer segments. The retinal detachment observed within the region of endothelial cell proliferation/migration in C3-injected retinas could occur as a result of leakage of fluid from the vasculature into the subretinal space. By 14 days after injection, all C3-injected eyes tested exhibited significant levels of leakiness.

Many AMD patients present initially with pigmentary changes in the RPE, manifesting as areas of both hyperpigmen-

tation and hypopigmentation.⁴⁰ In approximately 40% of patients with advanced AMD, this progresses to geographic atrophy in which there are areas of RPE cell loss through which choroidal vessels are visible, with an overlying area of photoreceptor degeneration. A loss of RPE cells and pigmentation is observed in C3-injected retinas, and a loss of photoreceptor outer segments is observed in the region of endothelial cell proliferation. Transdifferentiating and migrating RPE cells have been observed in intimate association with choroidal neovascular membranes of AMD patients.⁴¹ RPE cells have also been shown to migrate into the retina in proliferative vitreoretinopathy.^{31,42} In C3-injected retinas, pigmentary deposits could be observed in close association with cells staining positively for the endothelial cell marker GSL I, and in some cases these cells could be observed penetrating the retina.

An increase in endothelial cell staining was also observed within the region of injection in the choroid (and in some cases the retina) of GFP-injected eyes, but these proliferating endothelial cells did not penetrate the RPE. Although we have shown previously that an Ad5-expressing red fluorescent protein from a CMV promoter does not cause CNV when injected into the subretinal space,⁴³ the titer of the virus injected in that study was approximately 20-fold less than that administered in this study. The increase in choroidal and retinal vascular endothelial cells in GFP-injected mice is, perhaps, not surprising considering the increase in VEGF mRNA levels observed in GFP-injected mice compared with those of uninjected mice.

Increased VEGF has been observed in the eyes of AMD patients, and inhibitors of VEGF and VEGF receptors are highly effective in controlling and reducing exudative disease.⁴⁴ The anaphylatoxins C3a and C5a have been shown to induce VEGF in the mouse RPE.²³ The complex relationship between CNV development and angiogenic factors such as VEGF, bFGF, and HGF has been recently investigated in the laser-induced model of neovascularization. Of the three factors studied, VEGF was the last to be upregulated, implying a less significant role in early CNV development.⁴⁵ An increase in VEGF expression was observed in C3-injected eyes 3 days after injection but could not be attributed to C3 expression because a similar increase was observed in GFP-injected eyes. This increase in VEGF expression was not detectable in C3-injected retinas at the 8-day time point. The decline in VEGF mRNA levels observed at 8 days after injection could have been the result of significant changes in VEGF-producing cells, such as the RPE and Müller cells.⁴⁶ Although the increase in VEGF expression was not sufficient to explain the phenotype observed in C3-injected retinas, we cannot exclude a role for this growth factor in the development of the phenotype. Indeed, a potentially limiting feature of this model is that it is likely that the adenovirus itself contributes to the development of the pathology of AdcmvC3-injected retinas. AdcmvGFP-injected eyes had significantly increased endothelial cell proliferation in the choroid and retina compared with uninjected eyes. In addition, similar levels of C3 expression were observed at the 3-day time point but not the 8-day time point in both GFP- and C3-injected mice. This may not be unexpected considering that activation of the mouse complement has been observed previously for adenovirus.⁴⁷

Patients with either exudative AMD or with geographic atrophy show reduced cone and rod function as measured by ERG.⁴⁸ In one study, the reduction in scotopic a- and b-wave amplitudes was observed to correlate with increasing light intensity.⁴⁹ In our study, C3-injected eyes were observed to have significantly reduced a-wave amplitudes, as measured by scotopic ERG, at the higher light intensity but not at the lower light intensity. In addition, b-wave amplitudes were seen to be reduced at both light intensities when compared with both GFP-injected and uninjected mice. This reduction in retinal

function was consistent with the loss of photoreceptor segments observed in C3-injected mice. Loss of outer segments could be attributed to vascular leakage or deposition of the MAC complex, which was observed on the remnant segments. It is worth noting that deposition of MAC at sublytic concentrations has been associated with the inhibition of apoptosis, providing a possible explanation for the absence of TUNEL staining in AdcmvC3-injected retinas.⁵⁰ No significant loss in ERG amplitudes was observed in GFP-injected mice compared with uninjected mice.

Activation of Müller cells (reactive gliosis) is a common feature of insults to the retina,³⁶ including retinal detachment. In fact, Müller cells have been shown to play a pivotal role in retinal detachment associated with fibrocontractive disorders such as PVR and proliferative diabetic retinopathy (PDR).⁵¹ Because of the intimate relationship between Müller cell processes and retinal blood vessels, increased vascular permeability is a concern during reactive gliosis. In addition, in human retinas, distribution of the C3a receptor is consistent with its presence on Müller cells.⁵² Altered expression and distribution of the intermediate filament protein GFAP, consistent with Müller cell activation, was observed in C3-injected eyes, and this was coincident with the region of detachment. To a lesser extent, a redistribution of GFAP was also seen in GFP-injected compared with uninjected eyes. This is perhaps not unexpected given the retinal detachment caused by a subretinal injection.

Although retinal detachment was variable in GFP-injected eyes, with some eyes showing little or no detachment, extensive retinal detachment was a consistent feature of C3-injected eyes. The changes we observed in GFAP expression and localization in the AdcmvC3-injected eyes, as well as the loss of photoreceptor outer segments, have been observed previously in models of retinal detachment.³¹ However, we have shown that the proliferation of endothelial cells and the disruption of the RPE layer observed in AdcmvC3-injected mice cannot be explained by retinal detachment alone. We have not been able to determine whether the detachment is a primary effect of C3 expression or a downstream effect of endothelial cell proliferation or disruption of the RPE layer. It is possible that exogenous C3 expression may not induce retinal detachment but could prevent efficient reattachment subsequent to subretinal injection. We cannot, however, exclude the possibility that at least some of the features exclusive to C3-injected mice and not observed in GFP-injected mice (such as reduced ERGs and fluorescein leakage) occur as a result of this detachment. In future studies, we would hope to better understand the role of detachment in this model. Retinal detachment is a feature of a number of retinal diseases in which complement has been implicated, such as AMD, PVR, and PDR.

Although a number of mouse models of AMD have been described,^{53,54} many of these are transgenic mice that require considerable aging of the mouse in addition to other special treatments, such as a high-fat diet, to recapitulate some of the pathologic conditions observed in AMD eyes and are impractical for accelerated development of therapies for this disease. We have previously described an ex vivo model of human MAC deposition on murine RPE, which we have used to test complement regulators such as CD59 and CD55.^{55,56} Although the laser-induced and VEGF-overexpression models develop quickly (within days or weeks of insult), these models are primarily representative of the exudative form of the disease,^{57–60} although the laser-induced CNV model has shown potential in elucidating the role of complement in CNV.^{20,37} Local increased expression of C3 in the mouse retina using an adenovirus not only recapitulates many of the pathologic conditions observed in AMD eyes—neovascularization, increased vascular permeability, RPE atrophy, hypopigmentation, retinal detachment, photoreceptor degener-

ation, and reduced retinal function—it does so within 1 to 2 weeks of virus administration. Given the range of abnormalities recapitulated and the time course of development, this model may be useful in further elucidating the role of complement not only in AMD but in other retinal diseases such as PVR and PDR and in the development of therapies for complement-mediated retinal diseases such as AMD.

References

- Gehrs KM, Jackson JR, Brown EN, Allikmets R, Hageman GS. Complement, age-related macular degeneration and a vision of the future. *Arch Ophthalmol*. 2010;128:349–358.
- Klein ML, Ferris FL 3rd, Armstrong J, et al. Retinal precursors and the development of geographic atrophy in age-related macular degeneration. *Ophthalmology*. 2008;115:1026–1031.
- Johnson LV, Leitner WP, Staples MK, Anderson DH. Complement activation and inflammatory processes in drusen formation and age related macular degeneration. *Exp Eye Res*. 2001;73:887–896.
- Johnson LV, Ozaki S, Staples MK, Erickson PA, Anderson DH. A potential role for immune complex pathogenesis in drusen formation. *Exp Eye Res*. 2000;70:441–449.
- Mullins RF, Aptsiauri N, Hageman GS. Structure and composition of drusen associated with glomerulonephritis: implications for the role of complement activation in drusen biogenesis. *Eye (Lond)*. 2001;15:390–395.
- Mullins RF, Russell SR, Anderson DH, Hageman GS. Drusen associated with aging and age-related macular degeneration contain proteins common to extracellular deposits associated with atherosclerosis, elastosis, amyloidosis, and dense deposit disease. *FASEB J*. 2000;14:835–846.
- Edwards AO, Ritter R 3rd, Abel KJ, Manning A, Panhuysen C, Farrer LA. Complement factor H polymorphism and age-related macular degeneration. *Science*. 2005;308:421–424.
- Hageman GS, Anderson DH, Johnson LV, et al. A common haplotype in the complement regulatory gene factor H (HF1/CFH) predisposes individuals to age-related macular degeneration. *Proc Natl Acad Sci U S A*. 2005;102:7227–7232.
- Haines JL, Hauser MA, Schmidt S, et al. Complement factor H variant increases the risk of age-related macular degeneration. *Science*. 2005;308:419–421.
- Gold B, Merriam JE, Zernant J, et al. Variation in factor B (BF) and complement component 2 (C2) genes is associated with age-related macular degeneration. *Nat Genet*. 2006;38:458–462.
- Yates JR, Sepp T, Matharu BK, et al. Complement C3 variant and the risk of age-related macular degeneration. *N Engl J Med*. 2007;357:553–561.
- Montes T, Tortajada A, Morgan BP, Rodriguez de Cordoba S, Harris CL. Functional basis of protection against age-related macular degeneration conferred by a common polymorphism in complement factor B. *Proc Natl Acad Sci U S A*. 2009;106:4366–4371.
- Maller JB, Fagerness JA, Reynolds RC, Neale BM, Daly MJ, Seddon JM. Variation in complement factor 3 is associated with risk of age-related macular degeneration. *Nat Genet*. 2007;39:1200–1201.
- Reynolds R, Hartnett ME, Atkinson JP, Giclas PC, Rosner B, Seddon JM. Plasma complement components and activation fragments: associations with age-related macular degeneration genotypes and phenotypes. *Invest Ophthalmol Vis Sci*. 2009;50:5818–5827.
- Gerl VB, Bohl J, Pitz S, Stoffelns B, Pfeiffer N, Bhakdi S. Extensive deposits of complement C3d and C5b-9 in the choriocapillaris of eyes of patients with diabetic retinopathy. *Invest Ophthalmol Vis Sci*. 2002;43:1104–1108.
- Zhang J, Gerhardinger C, Lorenzi M. Early complement activation and decreased levels of glycosylphosphatidylinositol-anchored complement inhibitors in human and experimental diabetic retinopathy. *Diabetes*. 2002;51:3499–3504.
- Baudouin C, Fredj-Reygrobellet D, Gordon WC, et al. Immunohistologic study of epiretinal membranes in proliferative vitreoretinopathy. *Am J Ophthalmol*. 1990;110:593–598.
- Stasi K, Nagel D, Yang X, et al. Complement component 1Q (C1Q) upregulation in retina of murine, primate, and human glaucomatous eyes. *Invest Ophthalmol Vis Sci*. 2006;47:1024–1029.

19. Tezel G, Yang X, Luo C, et al. Oxidative stress and the regulation of complement activation in human glaucoma. *Invest Ophthalmol Vis Sci.* 2010;51:5070–5082.
20. Bora NS, Kaliappan S, Jha P, et al. CD59, a complement regulatory protein, controls choroidal neovascularization in a mouse model of wet-type age-related macular degeneration. *J Immunol.* 2007;178:1783–1790.
21. Bora NS, Kaliappan S, Jha P, et al. Complement activation via alternative pathway is critical in the development of laser-induced choroidal neovascularization: role of factor B and factor H. *J Immunol.* 2006;177:1872–1878.
22. Bora PS, Sohn JH, Cruz JM, et al. Role of complement and complement membrane attack complex in laser-induced choroidal neovascularization. *J Immunol.* 2005;174:491–497.
23. Nozaki M, Raisler BJ, Sakurai E, et al. Drusen complement components C3a and C5a promote choroidal neovascularization. *Proc Natl Acad Sci U S A.* 2006;103:2328–2333.
24. Coffey PJ, Gias C, McDermott CJ, et al. Complement factor H deficiency in aged mice causes retinal abnormalities and visual dysfunction. *Proc Natl Acad Sci U S A.* 2007;104:16651–16656.
25. Lundh von Leithner P, Kam JH, Bainbridge J, et al. Complement factor H is critical in the maintenance of retinal perfusion. *Am J Pathol.* 2009;175:412–421.
26. Rohrer B, Guo Y, Kunchithapatham K, Gilkeson GS. Eliminating complement factor D reduces photoreceptor susceptibility to light-induced damage. *Invest Ophthalmol Vis Sci.* 2007;48:5282–5289.
27. Kuehn MH, Kim CY, Jiang B, Dumitrescu AV, Kwon YH. Disruption of the complement cascade delays retinal ganglion cell death following retinal ischemia-reperfusion. *Exp Eye Res.* 2008;87:89–95.
28. Markiewski MM, Lambris JD. The role of complement in inflammatory diseases from behind the scenes into the spotlight. *Am J Pathol.* 2007;171:715–727.
29. Cashman SM, Sadowski SL, Morris DJ, Frederick J, Kumar-Singh R. Intercellular trafficking of adenovirus-delivered HSV VP22 from the retinal pigment epithelium to the photoreceptors—implications for gene therapy. *Mol Ther.* 2002;6:813–823.
30. Cashman SM, Morris DJ, Kumar-Singh R. Adenovirus type 5 pseudotyped with adenovirus type 37 fiber uses sialic acid as a cellular receptor. *Virology.* 2004;324:129–139.
31. Fisher SK, Lewis GP, Linberg KA, Verardo MR. Cellular remodeling in mammalian retina: results from studies of experimental retinal detachment. *Prog Retin Eye Res.* 2005;24:395–431.
32. Bednarczyk JL, Capra JD. Post-translational processing of the murine third component of complement. *Scand J Immunol.* 1988;27:83–95.
33. Van den Berg CW, Van Dijk H, Capel PJ. Rapid isolation and characterization of native mouse complement components C3 and C5. *J Immunol Methods.* 1989;122:73–78.
34. Yannuzzi LA, Negrão S, Iida T, et al. Retinal angiomatous proliferation in age-related macular degeneration. *Retina.* 2001;21:416–434.
35. Ucuzian AA, Gassman AA, East AT, Greisler HP. Molecular mediators of angiogenesis. *J Burn Care Res.* 2010;31:158–175.
36. Bringmann A, Pannicke T, Grosche J, et al. Müller cells in the healthy and diseased retina. *Prog Retin Eye Res.* 2006;25:397–424.
37. Rohrer B, Long Q, Coughlin B, et al. A targeted inhibitor of the alternative complement pathway reduces angiogenesis in a mouse model of age-related macular degeneration. *Invest Ophthalmol Vis Sci.* 2009;50:3056–3064.
38. Wu G, Hu W, Shahsafai A, et al. Complement regulator CD59 protects against atherosclerosis by restricting the formation of complement membrane attack complex. *Circ Res.* 2009;104:550–558.
39. Benzaquen LR, Nicholson-Weller A, Halperin JA. Terminal complement proteins C5b-9 release basic fibroblast growth factor and platelet-derived growth factor from endothelial cells. *J Exp Med.* 1994;179:985–992.
40. Klein R, Klein BE, Knudtson MD, Meuer SM, Swift M, Gangnon RE. Fifteen-year cumulative incidence of age-related macular degeneration: the Beaver Dam Eye Study. *Ophthalmology.* 2007;114:253–262.
41. Lopez PF, Sippy BD, Lambert HM, Thach AB, Hinton DR. Trans-differentiated retinal pigment epithelial cells are immunoreactive for vascular endothelial growth factor in surgically excised age-related macular degeneration-related choroidal neovascular membranes. *Invest Ophthalmol Vis Sci.* 1996;37:855–868.
42. Hiscott P, Sheridan C, Magee RM, Grierson I. Matrix and the retinal pigment epithelium in proliferative retinal disease. *Prog Retin Eye Res.* 1999;18:167–190.
43. Cashman SM, Bowman L, Christofferson J, Kumar-Singh R. Inhibition of choroidal neovascularization by adenovirus-mediated delivery of short hairpin RNAs targeting VEGF as a potential therapy for AMD. *Invest Ophthalmol Vis Sci.* 2006;47:3496–3504.
44. Ozkiris A. Anti-VEGF agents for age-related macular degeneration. *Expert Opin Ther Pat.* 2010;20:103–118.
45. Hu W, Criswell MH, Fong SL, et al. Differences in the temporal expression of regulatory growth factors during choroidal neovascular development. *Exp Eye Res.* 2009;88:79–91.
46. Saint-Geniez M, D'Amore PA. Development and pathology of the hyaloid, choroidal and retinal vasculature. *Int J Dev Biol.* 2004;48:1045–1058.
47. Tian J, Xu Z, Smith JS, Hofherr SE, Barry MA, Byrnes AP. Adenovirus activates complement by distinctly different mechanisms in vitro and in vivo: indirect complement activation by virions in vivo. *J Virol.* 2009;83:5648–5658.
48. Gerth C. The role of the ERG in the diagnosis and treatment of age-related macular degeneration. *Doc Ophthalmol.* 2009;118:63–68.
49. Walter P, Widder RA, Luke C, Konigsfeld P, Brunner R. Electrophysiological abnormalities in age-related macular degeneration. *Graefes Arch Clin Exp Ophthalmol.* 1999;237:962–968.
50. Cole DS, Morgan BP. Beyond lysis: how complement influences cell fate. *Clin Sci.* 2003;104:455–466.
51. Guidry C. The role of Müller cells in fibrocontractive retinal disorders. *Prog Retin Eye Res.* 2005;24:75–86.
52. Vogt SD, Barnum SR, Curcio CA, Read RW. Distribution of complement anaphylatoxin receptors and membrane-bound regulators in normal human retina. *Exp Eye Res.* 2006;83:834–840.
53. Edwards AO, Malek G. Molecular genetics of AMD and current animal models. *Angiogenesis.* 2007;10:119–132.
54. Elizabeth Rakoczy P, Yu MJ, Nusinowitz S, Chang B, Heckenlively JR. Mouse models of age-related macular degeneration. *Exp Eye Res.* 2006;82:741–752.
55. Ma K, Cashman S, Sweigard JH, Kumar-Singh R. Decay accelerating factor (CD55) mediated attenuation of complement: therapeutic implications for age-related macular degeneration. *Invest Ophthalmol Vis Sci.* 2010;51:6776–6783.
56. Ramo K, Cashman SM, Kumar-Singh R. Evaluation of adenovirus-delivered human CD59 as a potential therapy for AMD in a model of human membrane attack complex formation on murine RPE. *Invest Ophthalmol Vis Sci.* 2008;49:4126–4136.
57. Baffi J, Byrnes G, Chan CC, Csaky KG. Choroidal neovascularization in the rat induced by adenovirus mediated expression of vascular endothelial growth factor. *Invest Ophthalmol Vis Sci.* 2000;41:3582–3589.
58. Grossniklaus HE, Kang SJ, Berglin L. Animal models of choroidal and retinal neovascularization. *Prog Retin Eye Res.* 2010;29:500–519.
59. Spilbury K, Garrett KL, Shen WY, Constable IJ, Rakoczy PE. Overexpression of vascular endothelial growth factor (VEGF) in the retinal pigment epithelium leads to the development of choroidal neovascularization. *Am J Pathol.* 2000;157:135–144.
60. Wang F, Rendahl KG, Manning WC, Quiroz D, Coyne M, Miller SS. AAV-mediated expression of vascular endothelial growth factor induces choroidal neovascularization in rat. *Invest Ophthalmol Vis Sci.* 2003;44:781–790.